academicJournals

Vol. 7(6), pp. 58-64, June, 2015
DOI: 10.5897/JGMR2015. 0224
Article Number: 2EC0D8A53576
ISSN 2006 – 9766

http://www.academicjournals.org/JGMR

Journal of Geology and Mining Research

Full Length Research Paper

On the representative elementary volumes of clay rocks at the mesoscale

Lukas M. Keller

Zürich University of Applied Sciences, Winterthur, Switzerland.

Received 13 April 2015; Accepted 26 May, 2015

Regarding clay rock at the mesoscale (that is, millimeter to centimeter), the structure of the porous clay matrix treated as continuum controls transport properties. Upscaling these mesoscale properties to the macroscale requires that representative elementary volumes (REVs) exists. The objective of this paper is to quantify the mesoscale REVs of the continuous clay matrix. Here, the REV is defined as the minimum volume for which the variance of the determined clay matrix content for one measured sample is sufficiently small. The calculations reveal a strong dependence of the size of REV on the clay matrix content. Assuming a relative error of 10% on the true bulk clay matrix content, the size of the REV increases from 200 microns to about 15 centimeter when the clay matrix content decreases from 0.7 to 0.13. The dependency of the size of REV on the clay matrix content is related to the grain size distribution of sand grains (e.g. carbonates and quartz). Sand grains in clay rocks with high sand contents have a wider grain size spectrum, which leads to a higher geometric complexity. This increases the size of the REV.

Key words: Representative elementary volume, opalinus clay, shales.

INTRODUCTION

The evaluation procedure whether clay rocks can be used as host rocks for repositories of nuclear waste or as reservoir rocks commonly involves transport modeling to predict the sealing behavior/reservoir quality of porous sedimentary rocks up to the repository/reservoir scale. Clay rock formations such as Opalinus Clay are typically heterogeneous from the microscopic through the mesoscopic to the macroscopic scale.

At the micrometer scale (that is, nanometer to micrometer) local variations of grain shape and size leads to an irregular pore space geometry, where pores are formed due to geometric incompatibilities along grain boundaries of clay platelets (Keller et al., 2013). These pores are commonly referred to as intergranular pores, which fundamentally control the flow properties of clay rocks. Moving up to the mesoscale (that is, millimeter to centimeter), layers composed of clay-rich domains may alternate with layers rich in non-clayey materials such as carbonates and quartz. Different content of non-clayey material likely affects the ability to store and transmit fluids and layers therefore contrast in transport properties (Revil and Cathles, 1999).

This is supported by the fact that nanoporosity in non-clayey components (carbonates) is low and the pore space consists of isolated pore objects, which are not connected (Keller et al., 2013). In a hierarchical upscaling

*E-mail: kelu@zhaw.ch . Tel: 0041 58 934 7778. Fax 0041 58 935 7837.

concept, microscopic properties related to different constituents (e.g. porous clay matrix) can be used to determine mesoscopic transport properties, which themselves can then be upscaled to the macroscale of geological models. Upscaling of transport properties using simulation tools is subject to the condition that inhomogenous rock constituents can be replaced with an equivalent homogenous material using a continuum description. The prerequisite for the use of a continuum description of rock constituents is the existence of the so-called representative elementary volumes (REVs). The REVs may be regarded as the smallest volumes that must be measured to determine a certain material property with an acceptable accuracy so that the determined value is representative for the whole (Kanit et al., 2003).

This definition is based on the idea that material properties are constant over certain length scales. If REVs of a property (e.g. porosity) exist they limit the length range, in which the continuum description of certain rock constituent is valid. Regarding clay rocks at the micrometer scale, the REV of porosity in the clay rich matrix is on the order of 100s of micrometers, which is about one order of magnitude larger than the typical length of the pore paths but is several orders of magnitude larger than the pore radii (Keller et al., 2011; Keller et al., 2013).

Similar REVs of porosity were determined for different samples, which imply that REV of porosity really exists and that the porous clay matrix can be treated as a continuum on the mesoscale. Hence, a clay rock at the mesoscale consists essentially of a permeable porous clayey matrix with interdispersed and non-permeable non-clayey grains. In such a case, transport properties of clay rocks depend on the volume fraction and geometrical properties of the clay matrix (Revil and Cathles, 1999). At the mesoscale the clay matrix content varies locally, which may best be illustrated by the presence of a sediment layering. In such cases, individual layers can be described as a continuum provided the minimum size of the local mesoscale REV is smaller than the thickness of the layers.

Regarding the overall layering, a REV likely exists if the layering follows a regular pattern. In case of a gradient in clay matrix content a REV may not exist at all. In this report we determine the size of the mesoscale REV related to the clay matrix treated as a continuum. The calculations are based on mesostructures, which were reconstructed on the base of synchrotron X-ray computed tomography (XCT). Then, the clay matrix content was measured in sub-samples of different sizes and for a number of realizations. These data sets are then used to determine the minimum size of material volume that must be analyzed to determine averaged bulk clay matrix content for a given error (Kanit et al., 2003). The calculations were done on the base of mesostructures, which are related to different clay matrix contents and that way unrevealed the relationship between the size of the REV and the clay matrix content.

METHODS

Samples

The determination of the REV is based on microstructural reconstructions, which were presented by Keller et al. (in pres.) and are displayed in Figure 1. Two out of the three samples are from the Schlattingen borehole SLA-1. The location of the borehole is in the Swiss Molasse basin near the town of Schaffhausen. The sedimentary sequence at SLA-1 includes marine limestones, marls and shales, which are unconformably covered by tertiary rock of the Alpine Molasse. Miocene thrusting related to the formation of the Jura Mountain did not affect rocks at SLA-1. Sample BD-7 is calcareous marl taken at a depth of 781 m. Sample Opa-3 was taken from Opalinus Clay unit and is an argillaceous marlstone taken at depth of 837 m. In order to cover a wider range of clay contents and related microstructures a third sample BWS was taken at Mont Terri rock laboratory in northwestern Switzerland (Bossart and Thury, 2008). This sample contains the highest content of non-clayey grains and was taken from sandy facies of Opalinus Clay. Clay matrix contents of the samples are documented in Table 1.

Input data

The segmented images from XCT were transformed into binary images, in which the clay matrix was set to white and the remaining area to black. Segmentation quality of our image processing workflow is discussed in Keller et al. (in press.). The resulting images are two-dimensional arrays of one's (white) and zeros (black). The images were then read into three-dimensional arrays of 0's and 1's, in which the 1's indicate the clay matrix. For the statistical analysis the analyzed volume was subdivided into a regular cubic grid/lattice, in which each cell has an edge length L that corresponds to a certain number of voxels. Then, the clay matrix content was measured for each cell.

This procedure was applied to grids with different grid constants (cells with different edge length L). This yielded different sets of measured clay matrix contents corresponding to different sample sizes L, which were then used as input for the calculation of the local clay matrix phase distribution and the calculation of the REV. Note, the edge length of the analyzed volumes are not integer multiples of the chosen grid constants, which led to residual volumes. These residual volumes were too small to be subdivided into measuring cells and were thus not considered in the calculations. In addition, the residual volumes were not the same for each grid constant, which led to differences in the total analyzed volumes related to each cell edge length L.

Local clay matrix phase distribution

To characterize the heterogeneity of the material we followed the approach outlined in Hilfer 1991; Biswal et al. 1998; Hu and Stroeven 2005; Hilfer and Helmig 2004; Cosenza et al. 2015. Based on different sets of measured clay matrix contents the local clay matrix content distribution can be calculated using the relation

$$\mu(\phi, L) = \frac{1}{m}\sum_{i=1}^{m} \delta(\phi - \phi(x_i, L))$$

where m is number of measurements for a specific sample size L

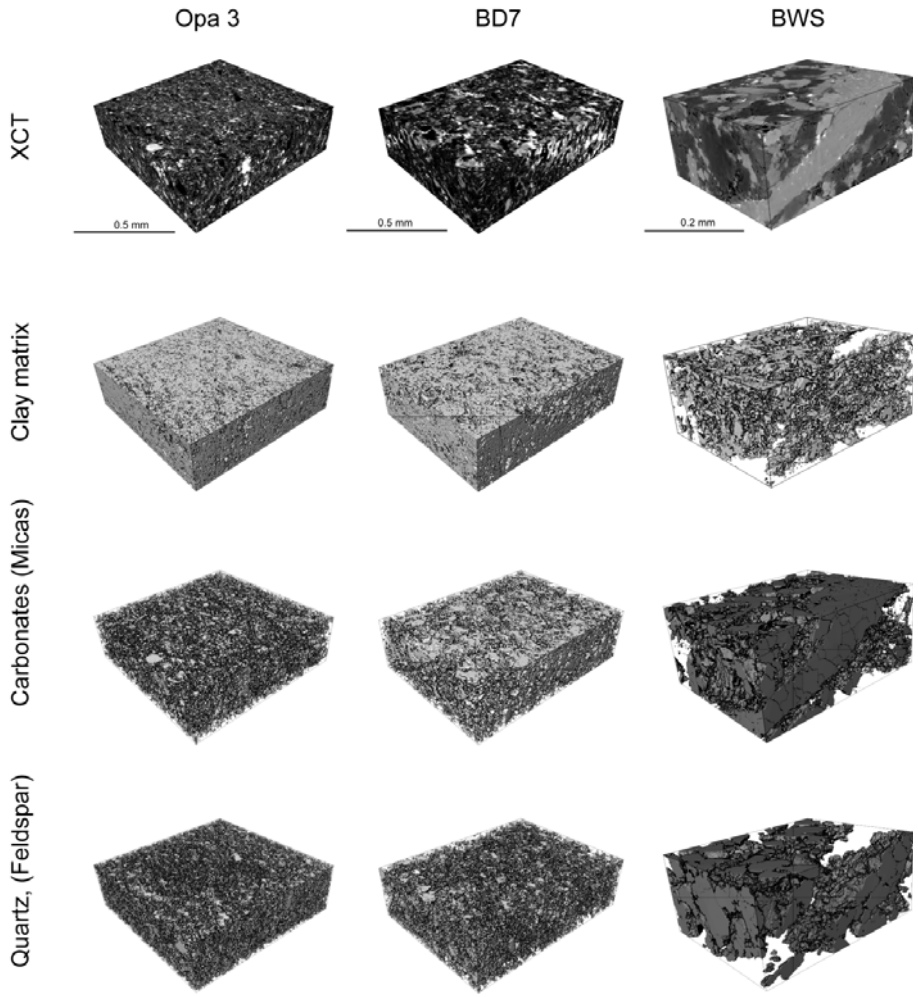

Figure 1. Reconstructed microstructures of major components (rows) of the analyzed samples (columns). XCT refers to the analyzed volume (see also Table 1).

and $\delta(t)$ denotes the delta function (Keller et al., 2013). The function $\mu(\phi,L)$ is a measure for the probability to find the local clay matrix content ϕ in a cell with side length L. Here, the local clay matrix content distribution was evaluated for 8 different cell sizes, which represent sub-samplings from the same set of tomographic data.

Representative elementary volume of clay matrix phase

On the millimeter scale a clay rock can be considered as a two-constituent mixture consisting of a permeable clay matrix and non-permeable non-clayey grains. In such a case, transport properties depend on the amount of non-clayey grains, which are dispersed in the clay matrix (Revil and Cathles, 1999; Keller et al., in press).

In terms of continuum transport modeling, the REV corresponds to a sub-volume that is sufficient in size to capture enough of the geometric complexity necessary for obtaining appropriate homogenized clay-matrix/non-clayey-grains properties. The REV can be imagined as a cube in 3D space whose properties correspond to the ones of the bulk rock (Bear, 1993). Therefore, the REV represents the bulk rock mass in transport models on a large scale. Note, that the REV must not necessarily be the same for all parameters.

Local clay matrix distributions showed that the clay matrix possesses a certain spatial homogeneity on the 100s of micrometer scale (Keller et al., 2013). However, at this length scale the mean clay matrix content is still related to an error, which decreases asymptotically with increasing L as shown in Figure 2. In addition, the mean clay matrix content does not vary much in dependence of L as shown in Figure 2.

In sample BWS, a minor decrease of mean clay matrix content for larger L (Figure 2a) is likely related to different sizes of the total analyzed volumes related to each size of measuring cell (see paragraph methods). These results indicate that the true mean value of clay matrix content can be predicted from a sample size that is smaller than the REV and that only a sample of infinite size will produce an error-free measurement.

In this way of thinking, a realistic size of REV (that is, not too large), which can also be used for macroscopic modeling, should be calculated for an acceptable error. In what follows and in order to calculate the size of the REV for a given error we used the method, which is outlined by Kanit et al. (2003) and references therein. Based on classical sample theory, the relative error on the exact mean value of clay matrix content M (or volume fraction in general), obtained from N independent realizations of volume V, is given by:

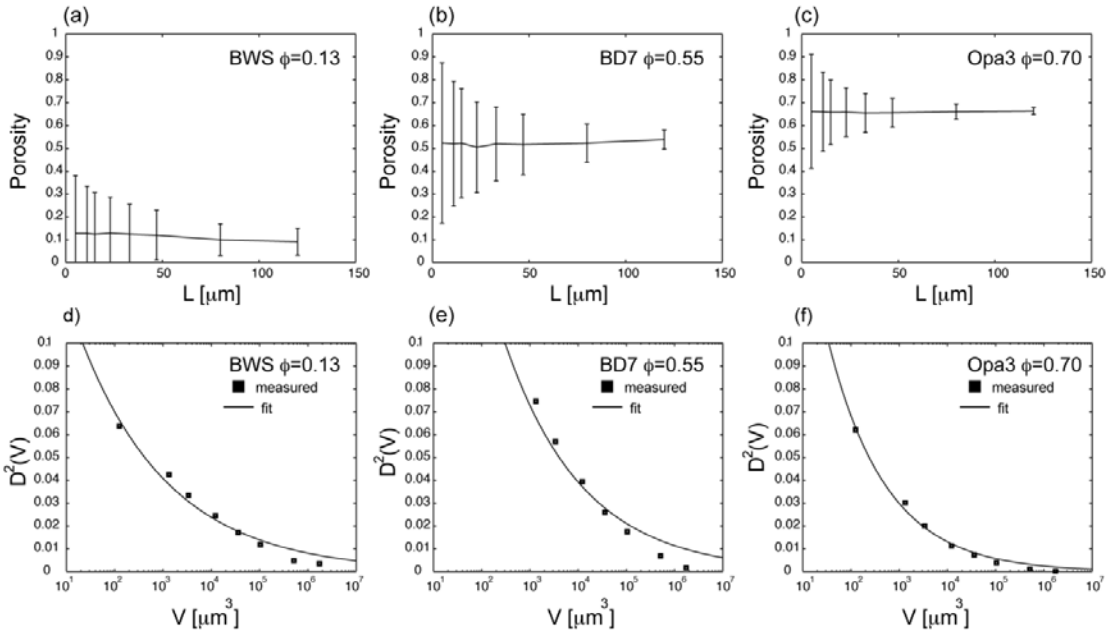

Figure 2. (a, b, c) Mean value of clay content and intervals of confidence versus size of measuring cells *L*. (d, e, f) variances of porosity versus volume of measuring cells.

$$\varepsilon_r = \frac{2D_\phi(V)}{M_\phi\sqrt{N}} \tag{1}$$

where *D(V)* is the standard deviation (the square root of variance). Following Kanit et al. (2003) the variance of clay matrix content may be given as:

$$D_\phi^2(V) = M_\phi(1-M_\phi)\left(\frac{A_3}{V}\right)^\alpha, \tag{2}$$

where A_3 is referred to as the integral range which gives information of the domain size of the clay matrix structure for which the clay matrix content in the measured volume *V* has good statistical representatives. If we plot the variance of clay matrix content vs. *L* in a log-log plot, the points are arranged on a straight line with a slope ≠ -1. According to Lantuejoul (1991), this points to an infinite integral range and because coefficient α controls the slope of the line we have $\alpha \neq 1$. In such a case, a power law in the form of Equation (2) with $\alpha \neq 1$ is proposed (Lantuejoul, 1991; Kanit et al., 2003). In the case of a finite integral range the slope is -1 with α = 1. Using Equation (1) in Equation (2) gives an expression for the smallest volume with a given relative error ε_r, *N* realization and the true mean value *M:*

$$V(N,\varepsilon_r) = \left(\frac{4(1-M_\phi)}{\varepsilon_r^2 N M_\phi}\right)^{1/\alpha} \cdot A_3 \tag{3}$$

The integral range A_3 for clay matrix was approximated by computing the variance $D^2(V)$ for the recorded clay matrix contents of the respective measuring cells of size *V*. Then, the integral range A_3 was obtained by fitting Equation (2) to our data as shown in Figure 2. Here one has the problem that the true mean value *M* of clay matrix content cannot be predicted from tomographic methods because they have been applied to volumes, of which sizes are far from infinite. The latter statement assumes that the true clay matrix content can be obtained from a clay rock body of infinite size, only. Here, we assumed that bulk volume fractions of clay matrix content that were determined are valid estimates of the true volume fractions. This is supported by the fact that calculated mean values do not vary much in dependence of *L* as depicted in Figure 2. The values of A_3, α and volume fractions for each sample are given in Table 1. Then, the size of the respective REV for each bulk clay matrix content can be calculated for a given precision of the mean value that results from different realizations *N* (that is, independent measure cells with the size of the REV).

RESULTS

Homogeneity of the clay matrix phase

In Figure 3 it can be seen that with increasing *L* the local clay content distributions μ of the samples change from a wide distribution to a distribution with a peak at the position of the bulk clay matrix content. With increasing clay content ϕ, the peak is increasingly more pronounced and spatial fluctuations in clay content decrease. Regarding sample Opa-3 the formation of single peak distribution starts at smaller samples sizes of *L* when compared to the other two samples. Furthermore, the peak width of sample Opa-3 is smaller when compared to samples BD-7 and BWS. The distributions of the latter

Table 1. Values of volume fractions of pores and clay content, integral range A_3 and coefficient α for different data sets obtained from different tomographic methods.

Sample	Volume (mm)	Clay matrix content ϕ	Integral range A_3 [μm^3]	Coefficient α	Figure
BWS	0.5×0.22×0.4	0.13	12.82	0.23	1
BD	1.0×0.8×0.3	0.55	10.50	0.27	1
Opa 3	0.8×0.8×0.3	0.70	4.37	0.36	1

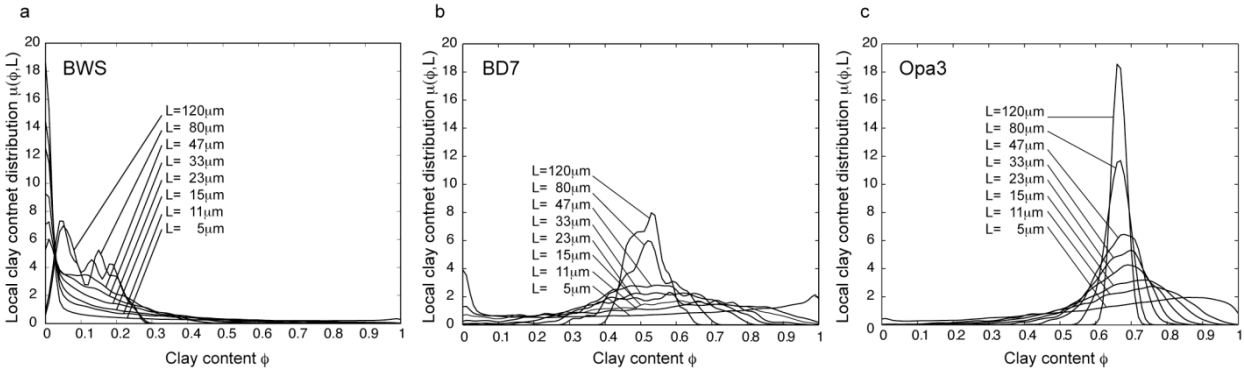

Figure 3. (a, b, c) Local clay matrix distributions calculated for different length *L* of measuring cell and on the base of XCT data

two samples indicate that spatial clay content fluctuations are still present on the hundreds of microns scale in samples with lower clay contents than 60 vol. %. In combination, these facts indicate that the clay matrix of sample Opa-3 is more homogenous than the one of samples BD-7 and BWS.

Apparently, homogeneity of the clay matrix in shales depends on clay content. Local clay content distributions μ can be regarded as a probability measure to find a local clay content within a cell or sample of certain size *L*. Regarding the clay content >~ 60 vol. % (that is, sample Opa-3) the development of a single peak occurs for cells with edge lengths *L* >~ 100 μm. Interestingly, Cosenza et al. (2015) have shown similar order of magnitude with a Callovo-Oxfordian clay rock, Figure 3, in Cosenza et al. 2015. This means that at few hundred-micron scale length, there is a high probability to find a local clay content that equals the bulk clay content, which in turn can only be true if the clay matrix, at this length scale, possesses a certain degree of homogeneity.

REV of clay matrix phase

Using expression (3), the REV of the clay matrix content can be calculated if parameter *N* is set to one (Kanit et al., 2003). Figure 4a shows calculated L_{REV} as a function of relative precisions ε_r. For a given relative error the size of the REV increases with decreasing clay matrix content. For example, accepting a relative error of 0.1, the size of the REV increases from 200 microns to about 15 cm when the clay matrix content decreases from 0.7 to 0.13. More practical would be a plot, which shows the size of REV as a function of the clay matrix content. Such a plot was constructed on the base of the data related to Figure 4a. Figure 4b allows an assessment of the REV for a given clay matrix content and relative error.

DISCUSSION

It was demonstrated that the size of the REV related to the microstructure of the continuum clay matrix depends on the volume fractions of the respective constituents. It was found that a decrease in clay matrix content is associated with a substantial increase of the size of the REV.

In part, this behavior is inherited in the definitions that were used to calculate the size of the REV, of which dependency on the volume fraction is such that the size of the REV increases with decreasing volume fraction ϕ. However, the size of the REV depends also on the integral range, of which value decreases towards higher clay matrix contents (Table 1). Furthermore, for larger sample sizes, the local variance of the clay matrix content is smaller in case of higher clay matrix contents. The systematic size variation of the integral range and local variance of the clay matrix content indicates that the

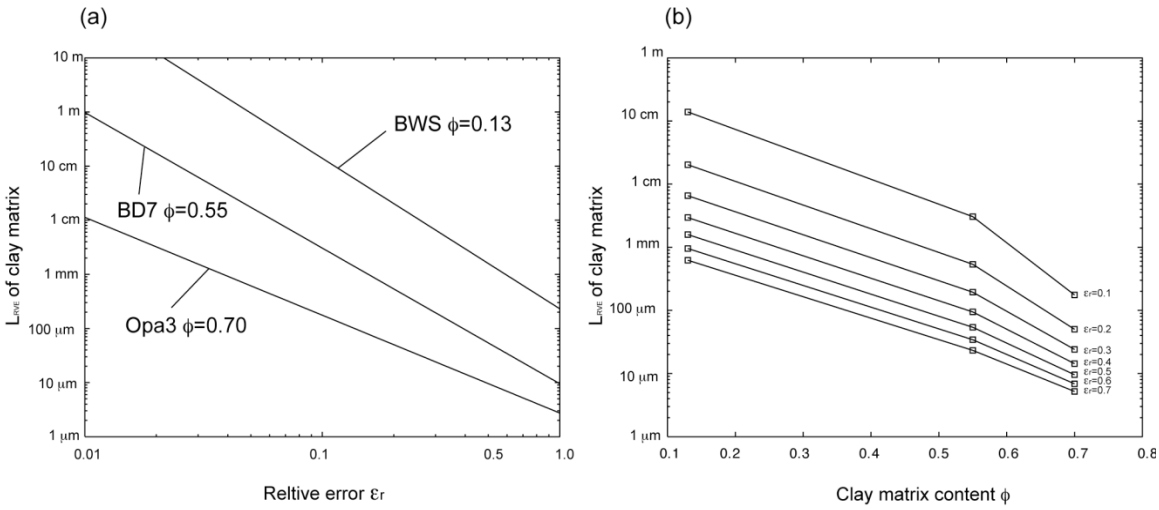

Figure 4. (a) REV of clay matrix vs. relative error ε_Y related to different clay matrix content. (b) REV of clay matrix vs. clay matrix content for a given relative error ε_Y.

morphological complexity increases with decreasing clay matrix content. This is supported by local clay matrix distributions, which indicate that the homogeneity of the clay matrix decreases with decreasing volume fraction.

Regarding the used approach, the coefficient α is considered as a measure for homogeneity and only a sample with $\alpha = 1$ can be considered to be representative at the mesoscale (Lantuejoul, 1991). In the present case α is clearly below 1, which indicates that none of the samples is representative in terms that the mean clay matrix content can be determined with high precision. However, the used approach also provides an idea of the error that can be expected if the mean clay matrix content is determined on the base of the presented samples. The samples have edge lengths of a few hundred microns, which in combination with Figure 4, implies that only sample Opa-3 provides information on the mean clay matrix content with an acceptable precision (relative error ~ 10%).

This finding is well in line with results related to local clay matrix distributions (Figure 3), showing that only sample Opa-3 develops a single peak distribution, whereas distributions of sample BD-7 and BWS are still associated with spatial fluctuations in clay matrix content at the hundred micron scale (curves develop several peaks). In addition, the coefficient α increases with increasing clay matrix content, which again indicates that the homogeneity increases with increasing clay matrix content.

The increasing morphological complexity towards lower clay matrix contents can be explained by realizing that the geometry of the clay matrix is in fact defined by the microstructure of non-clayey grains. The samples show a systematic relationship between clay content and grain size distributionof non-clayey mineral grains (Figures 1 and 5), which in case of carbonates is well pronounced and reveals that an increase in clay content is related to a decrease in grain-size spectrum of non-clayey grains.

In case of quartz, this trend is less pronounced but the low-clay content sample BWS shows a substantial higher grain size spectrum when compared to the other two samples. Hence, the investigated samples imply that clay rocks with low clay matrix contents contain more, larger and a larger size spectrum of non-clayey grains when compared to samples with higher clay matrix content. Hence, a higher geometric complexity of the non-clayey grains/clay matrix microstructure can be expected for clay rocks with low clay matrix contents, which then increases the size of the REV. However, it remains unclear if the observed correlation between the grain size spectrum of non-clay grains and the clay content is a generic trend, or merely a correlation related to the 3 investigated samples.

Continuum models are used to predict the behavior of radioactive waste deposits at various scales. Such methods assume that the host rock exists as a continuum, which in the case of clay matrix content means that it is homogenously distributed over a certain length scale. More specifically, the continuum assumption depends on the idea of a REV. The size of the REV is related to specific material properties and here we discussed the size of the REV related to the porous clay matrix treated as a continuum.

In a continuum description, the clay matrix is attributed with the porosity associated with the REV related to the micrometer scale. Thus, the presented size of REVs is expected to not differ much from the ones related to mesoscale flow properties such as permeability, which depend on the porosity. Furthermore, solute transport in clay rocks occurs by diffusion within the clay matrix and

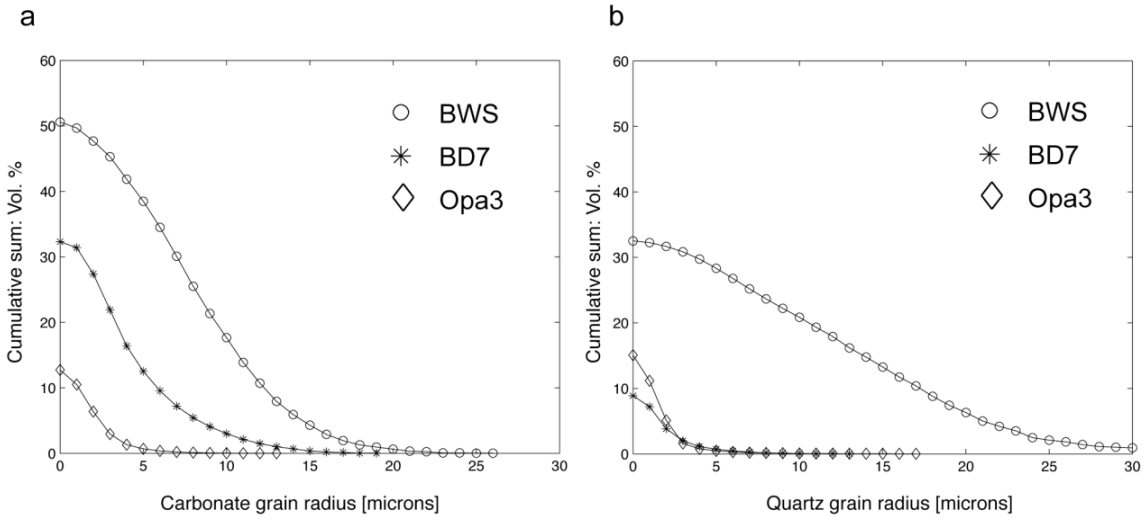

Figure 5. Grain size distribution of (a) carbonates and (b) tectosilicate grains.

thus, depends on volume fraction and geometric properties of the clay matrix phase (e.g. constrictivity, geometric tortuosity). Hence, it is expected that the REV of clay matrix will be on the same order of magnitude as the one related to the REV of diffusion. It should be noted that the results presented here are restricted to cases where the microstructure is homogenous over a certain length scale. In case of a continuous lateral change in clay matrix content, the determined REV (based on Figure 4) is only of local relevance.

Conclusion

The representative elementary volume of the clay matrix treated as a continuum and its dependence on clay content was addressed. It was demonstrated that homogeneity and the size of the REV of the clay matrix depend on clay content. This result is better understood from the perspective of non-clayey grains. An increase in the amount of non-clayey grains is associated with an increase in the grain size spectrum, which in combination results in an increase of geometric complexity and an increase of the sample size that must be analyzed to capture the geometric complexity of the sample. Assuming a relative error on the mean clay matrix content of 10% and for a clay matrix content of 0.13, the REV is on the order of 15 cm. The REV decreases substantially with increasing clay matrix content and reaches values of < 1 mm for clay contents of around 0.7. As a consequence, computational efforts attempting to calculate effective properties of transport properties, which depend on the clay matrix content, must be carried out on the base of system sizes, which consider the strong dependence of REV on clay matrix content.

Conflict of interest

The author has not declared any conflict of interest

REFERENCES

Bear J (1993). Modeling flow and contaminant transport in fractured rocks, Flow and contaminant transport in fractured rocks. Edited by J Bear, C Tsang, and M Ghislain, Academic Press, New York, pp. 1-37,

Biswal B, Manwart C, Hilfer R (1998). Three-dimensional local porosity analysis of porous media. Physica A 255:221-241.

Bossart P, Thury M (2008). Mont Terri Rock Laboratory: Project, Programme 1996-2007 and Results. Reports of the Swiss Geological Survey, No. 3.

Cosenza P, Pret D, Zamora M (2015). Effect of local clay distribution on the effective electrical conductivity of clay-rocks. J. Geophys. Res. 120:2169-9356 doi.org/10.1002/2014JB011429.

Hilfer R (1991). Geometric and dielectric characterization of porous media. Phys. Rev. 44:60-75.

Hilfer R, Helmig R (2004). Dimensional analysis and upscaling of two phase flow in porous media with piecewise constant heterogeneities. Adv. Water Resour. 27:1033-1040.

Hu J, Stroeven P (2005). Local analysis of pore structure in cement paste. Cem. Concr. Res. 35:233-242.

Kanit T, Forest S, Gailliet I, Mounoury V, Jeulin D (2003). Determination of the representative volume for random composites: statistical and numerical approach. Int. J. Solids Struct. 40:3647-3679.

Keller LM, Schuetz P, Gasser P, Holzer L (2013). Pore-space relevant for gas-permeability in Opalinus Clay: Statistical analysis of homogeneity, percolation and representative volume element. J. Geophys. Res. 118:1-14.

Keller LM, Holzer L, Wepf R, Gasser P (2011). 3D Geometry and topology of pore pathways in Opalinus clay: Implications for mass transport. Appl. Clay Sci. 52:85-95.

Keller LM, Hilger A, Manke I (in press.). Mesostructural effects on solute diffusion in Opalinus Clay. Appl. Clay Sci.

Lantuejoul Ch (1991). Ergodicity and integral range. J. Micros. 161:387-403.

Revil A, Cathles LM (1999). Permeability of shaly sands. Water Resour. Res. 35:651-662.